$\mathcal{R}$esearch in
$\mathcal{A}$stronomy and
$\mathcal{A}$strophysics

Long-term optical-infrared color variability of blazars [*]

Bing-Kai Zhang[1], Xiao-Shan Zhou[1], Xiao-Yun Zhao[1], Ben-Zhong Dai[2]

[1] Department of Physics, Fuyang Normal College, Fuyang 236041, China; *zhangbk@ihep.ac.cn*
[2] Department of Physics, Yunnan University, Kunming 650091, China

Abstract The long-term optical and infrared color variability of blazars has been inves-
tigated with the SMARTS monitoring data. The sample in this study consists of 49 flat
spectrum radio quasars and 22 BL Lac objects. The fractional variability amplitudes of
each source have been calculated in both optical R band and infrared J band. Overall,
the variability amplitudes of FSRQs are larger than those of BL Lac objects. The results
also suggest that the variability amplitude of most FSRQs is larger at lower energy band
(J band) than at higher one (R band), while the variability amplitude of BL Lacs are
larger at higher energy band. Two types of blazars both display color variation along with
the variability in brightness. However, they show different variation behaviors in general.
With the whole data set, 35 FSRQs exhibit redder-when-brighter trends, and 11 FSRQs
exhibit opposite trends; 11 BL Lacs follow bluer-when-brighter trends, and 7 BL Lacs
follow opposite trends. The examination in detail shows that there are 10 blazars showing
redder-when-brighter trend in their low state, and bluer-when-brighter or stable-when-
brighter trends in their high state. Some more complicated color behaviors have also been
detected in several blazars. The non-thermal jet emission and the thermal emission from
the accretion disc are employed to explain the observed color behaviors.

Key words: galaxies: active – BL Lacertae objects: general – quasars: general – methods:
statistical

1 INTRODUCTION

Blazars consist of flat spectrum radio quasars (FSRQs) and BL Lacertae objects (BL Lacs). They are
dominated by non-thermal continuum emission. The flux decreases along with the frequency increasing,
which approximately follows a power law. Measurements of the spectral energy distribution (SEDs)
play an important role in understanding the emission processes of blazars. Since blazars vary rapidly
and violently at all wavelengths from radio to γ-ray with time scales from minutes to years (Carini et
al. 1992; Arévalo et al. 2008; Ghosh et al. 2000; Ciprini et al. 2007; Chatterjee et al. 2012; Zhang et al.
2013; D'Ammando et al. 2013), the lack of simultaneous data at the various wavelengths is an obstacle
in the broadband study of blazars. Flux variations in blazars are usually accompanied by changes in the
spectral shape. Therefore, the analysis of spectral changes of blazars can put some strong constraints on
the physical processes that are responsible for these variations.

The spectral change can be characterized by the color change. Color variations in blazars have been
explored by several authors. For 28 radio-selected BL Lacs in Fan & Lin (2000), two showed flatter
spectra when getting brighter, while three showed opposite behavior. Vagnetti, Trevese & Nesci (2003)

---

found bluer-when-brighter (BWB) trends in the $BVRI$ bands for all 8 BL Lacs in their sample. Gu et al. (2006) found that 3 out of 5 BL Lacs exhibited significant BWB trends and 2 out of 3 FSRQs exhibited redder-when-brighter (RWB) trends. However, Gu & Ai (2011) showed that only one FSRQs is RWB in a sample of 29 SDSS FSRQs. Rani et al. (2010) found that 3 out of 6 BL Lacs tended to become bluer with increase in brightness, and 4 out of 6 FSRQs exhibited opposite trends. Ikejiri et al. (2011) found that 28 out of 32 well observed blazars showed BWB trend. Bonning et al. (2012) found that FSRQs had redder optical-infrared colors when they were brighter, while BL Lac objects showed no such trend. Gaur et al. (2012) suggested that 6 out of 10 BL Lacs followed the BWB trend, while all 6 BL Lacs in Sandrinelli, Covino & Treves (2014) showed no BWB trends. The color behaviors of some individual sources are also investigated in many disperse literatures (e.g. Raiteri et al. 2003; Papadakis et al. 2003; Hu et al. 2006; Wu et al. 2006, 2011; Dai et al. 2009; Zhang et al. 2010a; Dai et al. 2011; Fan et al. 2014).

BWB and RWB trends are two common well-observed behaviors in blazars. However, some complicated color phenomena have also been found in some cases. In general, there are five kinds of color behaviors: BWB in the whole data sets; RWB in the whole data sets; cycles or loop-like pattern; RWB at the low state while BWB at the high state (RWB to BWB); stable-when-brighter (SWB) or no correlation with brightness in the whole data sets (see Zhang et al. (2014) and references therein). Up to now, FSRQs and BL Lacs seem not to have universal features in color variations. The purpose of this paper is to investigate their color behaviors using a much larger sample of blazars with almost simultaneous measurements, and expect to provide results with higher confidence levels. The paper is organized as following: in Section 2, the infrared and optical data as well as their variations are described; in Section 3, the color behavior is studied; then the discussion and conclusions are given in Section 4.

2 INFRARED AND OPTICAL DATA & VARIABILITY

In order to investigate the statistics of the color behavior of blazars, we collect 71 blazars as well as 4 possible blazars from SMARTS sources. SMARTS program employs four meter-class telescopes (1.5-m, 1.3-m, 1.0-m and 0.9-m) of the Small and Moderate Aperture Research Telescope System (SMARTS) at Cerro Tololo Interamerican Observatory (CTIO) in Chile to observe the bright southern gamma-ray blazars on a regular cadence, at both optical and near-infrared wavelengths. Data reduction and analysis of SMARTS data have been described in Bonning et al. (2012). Table 1 lists our sample which comprises 49 FSRQs, 22 BL Lacs and 4 unidentified type sources. The first column gives the object name, the second column gives the spectral classification, the third one gives the monitoring duration in days, the fourth one gives the number of data points for color index calculation. Most of the sources are observed in B, V, R, J and K bands. On the whole, there are the most data points in R and J bands. So, these two bands have been selected to study color variations. However, the observations for each source are not uniform. Some objects have been observed for more than 2000 days, while some others have been observed for less than 100 days. Some sources have been well observed with hundreds of data points and some less than 10 data points.

In order to compare the amplitude of the variations in different blazars, and in different bands for the same blazar, we compute the fractional variability amplitude F_{var} (Vaughan et al. 2003), which represents the average amplitude of the observed variations as a percentage of the light curve mean. The fractional variability amplitude is defined as $F_{var} = \sqrt{(S^2 - <\varepsilon_{err}^2>)/<x>^2}$, where S^2 is the sample variance of the light curve, $<x>$ is the average flux and $<\varepsilon_{err}^2>$ is the mean of the squared measurement uncertainties. The F_{var} values of J and R bands are listed in the fifth and sixth columns of Table 1. In Fig. 1 we plot the F_{var} of R band versus that of J band for each object. It can be seen that the objects show great differences in variations. Most of the objects show significant variabilities. Several sources display extreme variability, such as AO 0235-164, with F_{var}=1.57 in J band and F_{var}=1.59 in R band. However, there are also a few sources showing weak variabilities, such as 3C 273, with $F_{var} = 0.06$ in J band and $F_{var} = 0.04$ in R band.

Fig. 2 plots the distribution of F_{var}s of R band and J band. On the whole, F_{var}s of R band have no significant difference with those of J band for all objects, which means that the variability amplitudes

Table 1 The Property of Variations of Optical and Infrared Data.

$Object$	$Class$	ΔT (day)	N	J_{Fvar}	R_{Fvar}	r_{J-R}	$Prob.$	r_{C-R}	$Prob.$	r_{C-J}	$Prob.$	$Behavior$
PMN 0017-0512	FSRQ	211	73	0.82±0.07	0.67±0.06	0.97	$< 10^{-9}$	0.67	$< 10^{-11}$	0.82	$< 10^{-9}$	RWB
PKS 0035-252	FSRQ	357	9	0.43±0.11	0.38±0.10	0.11	0.78	-0.49	0.18	0.81	8.0×10^{-3}	RWB
PKS 0208-512	FSRQ	2016	381	0.96±0.03	0.86±0.03	0.96	$< 10^{-9}$	0.30	2.7×10^{-9}	0.55	$< 10^{-9}$	RWB
4C+01.02	FSRQ	76	8	0.32±0.08	0.17±0.04	0.73	0.04	0.34	0.40	0.89	2.7×10^{-3}	RWB
AO 0235+164	FSRQ	1816	221	1.57±0.07	1.59±0.08	0.98	$< 10^{-9}$	0.21	2.1×10^{-3}	0.38	4.2×10^{-9}	RWB
PKS 0235-618	FSRQ	158	14	0.25±0.05	0.32±0.06	0.48	0.09	-0.72	3.9×10^{-3}	0.27	0.35	BWB
1RXS 0238-3116	BL Lac	654	20	0.20±0.03	0.29±0.05	-0.10	0.68	-0.87	7.7×10^{-7}	0.58	7.2×10^{-3}	BWB(RWB)
PKS 0250-225	FSRQ	90	50	0.40±0.04	0.40±0.04	0.85	$< 10^{-9}$	-0.26	0.07	0.29	0.04	None
PKS 0301-243	BL Lac	537	48	0.15±0.02	0.18±0.02	0.84	$< 10^{-9}$	-0.56	4.1×10^{-5}	-0.02	0.89	BWB
BG6 J0316+0904	BL Lac	783	12	0.16±0.03	0.25±0.05	0.92	2.3×10^{-5}	-0.82	9.7×10^{-4}	-0.54	0.07	BWB
PKS 0402-362	FSRQ	863	75	0.26±0.02	0.17±0.01	0.86	$< 10^{-9}$	0.34	2.5×10^{-3}	0.78	$< 10^{-9}$	RWB
PMN 0413-5332	FSRQ	763	11	0.48±0.12	0.10±0.06	-0.26	0.44	-0.49	0.12	0.97	9.0×10^{-7}	RWB
PKS 0422+004	BL Lac	498	11	0.42±0.09	0.44±0.09	0.99	1.5×10^{-8}	-0.28	0.40	-0.13	0.71	None
PKS 0426-380	FSRQ	419	163	0.35±0.02	0.34±0.02	0.92	$< 10^{-9}$	-0.18	0.02	0.22	4.9×10^{-3}	RWB
NRAO 190	FSRQ	236	15	0.86±0.16	0.77±0.14	0.94	1.7×10^{-7}	0.32	0.24	0.62	0.01	RWB
PKS 0454-234	FSRQ	847	286	0.61±0.03	0.68±0.03	0.99	$< 10^{-9}$	-0.62	$< 10^{-9}$	-0.48	$< 10^{-9}$	BWB
PKS 0454-46	FSRQ	1193	47	0.14±0.02	0.15±0.02	0.21	0.16	-0.61	5.6×10^{-6}	0.65	8.5×10^{-7}	RWB(BWB)
S3 0458-02	FSRQ	496	39	0.34±0.04	0.31±0.04	0.93	$< 10^{-9}$	0.12	0.45	0.48	1.9×10^{-3}	RWB
PKS 0502+049	FSRQ	309	36	0.52±0.06	0.34±0.04	0.76	9.4×10^{-8}	0.01	0.97	0.66	1.2×10^{-5}	RWB
PMN 0507-6104	FSRQ	816	6	0.61±0.18	0.66±0.19	0.75	0.09	-0.25	0.64	0.46	0.36	None
PKS 0528+134	FSRQ	2091	160	0.54±0.03	0.31±0.02	0.78	$< 10^{-9}$	0.23	4.1×10^{-3}	0.79	$< 10^{-9}$	RWB
PMN J0531-4827	–	1215	175	0.94±0.05	1.01±0.05	0.98	$< 10^{-9}$	-0.34	3.6×10^{-6}	-0.13	0.09	BWB
PKS 0537-441	FSRQ	1115	141	0.77±0.05	0.66±0.04	0.97	$< 10^{-9}$	0.16	0.05	0.40	1.1×10^{-6}	RWB
PMN J0623+3350	–	61	20	0.40±0.07	0.54±0.09	0.75	1.2×10^{-4}	-0.67	1.2×10^{-3}	-0.02	0.93	BWB
J0630.9-2406	BL Lac	827	18	0.21±0.04	0.12±0.02	0.37	0.14	-0.26	0.30	0.81	5.5×10^{-5}	RWB
PKS 0637-75	FSRQ	1193	72	0.09±0.01	0.07±0.01	0.30	0.01	-0.46	5.7×10^{-5}	0.72	$< 10^{-9}$	RWB(BWB)
PKS 0727-11	FSRQ	989	18	0.64±0.12	0.88±0.15	0.96	$< 10^{-9}$	-0.86	4.1×10^{-6}	-0.69	1.7×10^{-3}	BWB
PMN J0816-1311	BL Lac	843	21	0.22±0.03	0.23±0.04	0.97	$< 10^{-9}$	-0.36	0.10	-0.11	0.62	None
PKS 0818-128	BL Lac	826	20	0.23±0.04	0.36±0.06	0.53	0.02	-0.76	1.1×10^{-4}	0.16	0.51	BWB
BZQ J0850-1213	FSRQ	1206	97	0.55±0.04	0.53±0.04	0.91	$< 10^{-9}$	-0.21	0.04	0.21	0.04	None
OJ 287	BL Lac	2203	364	0.42±0.02	0.41±0.02	0.92	$< 10^{-9}$	-0.04	0.49	0.35	$< 10^{-9}$	RWB
PKS 1004-217	FSRQ	1087	81	0.20±0.02	0.14±0.01	-0.12	0.29	-0.72	$< 10^{-9}$	0.77	$< 10^{-9}$	RWB(BWB)
PKS 1056-113	BL Lac	728	43	0.37±0.04	0.43±0.05	0.97	$< 10^{-9}$	-0.35	0.02	-0.10	0.52	None
PKS 1124-186	FSRQ	351	34	0.34±0.04	0.34±0.04	1.00	$< 10^{-9}$	0.54	9.5×10^{-4}	0.60	2.0×10^{-4}	RWB
PKS 1127-14	FSRQ	1103	37	0.21±0.03	0.17±0.02	-0.12	0.49	-0.62	4.6×10^{-5}	0.85	$< 10^{-9}$	RWB(BWB)
PKS 1144-379	FSRQ	1115	128	0.56±0.04	0.65±0.04	0.93	$< 10^{-9}$	-0.66	$< 10^{-9}$	-0.34	6.9×10^{-5}	BWB
QSO B1212+078	BL Lac	942	9	0.07±0.02	0.12±0.03	0.47	0.21	-0.78	0.01	0.18	0.63	BWB
3C 273	FSRQ	2156	287	0.06±0.00	0.04±0.00	0.14	0.02	-0.54	$< 10^{-9}$	0.76	$< 10^{-9}$	RWB(BWB)
PKS 1244-255	FSRQ	1032	107	0.55±0.04	0.48±0.03	0.98	$< 10^{-9}$	0.69	$< 10^{-9}$	0.81	$< 10^{-9}$	RWB
3C 279	FSRQ	2207	447	0.68±0.02	0.72±0.02	0.99	$< 10^{-9}$	-0.46	$< 10^{-9}$	-0.33	$< 10^{-9}$	BWB
PKS 1329-049	FSRQ	376	11	0.24±0.08	0.48±0.11	0.08	0.82	-0.73	0.01	0.62	0.04	BWB
PKS 1335-127	FSRQ	1077	54	0.91±0.09	0.87±0.08	0.95	$< 10^{-9}$	0.10	0.47	0.42	1.6×10^{-3}	RWB
PKS B1406-076	FSRQ	2201	180	0.61±0.03	0.44±0.02	0.80	$< 10^{-9}$	0.14	0.06	0.71	$< 10^{-9}$	RWB
PKS B1424-418	FSRQ	765	278	0.71±0.03	0.74±0.03	0.99	$< 10^{-9}$	-0.38	$< 10^{-9}$	-0.26	1.3×10^{-5}	BWB
PKS 1508-05	FSRQ	745	25	0.20±0.03	0.10±0.02	0.25	0.22	-0.27	0.20	0.86	2.7×10^{-8}	RWB

of R and J band in blazars are comparable. Ghosh et al. (2000) suggested that it may not be correct to generalize that the amplitude of the variation in blazars is systematically larger at higher frequency. However, as can be seen in Fig. 1, F_{var}s of J band are generally larger than those of R band for most of FSRQs (with $prob. = 0.025$), while F_{var}s of J band are, in general, smaller than those of R band for most of BL Lacs (with $prob. = 0.033$). Bonning et al. (2012) also found that 8 out of 9 FSRQs are more variable in J band than B band. As can also be seen in Fig. 1, the F_{var}s of FSRQs seem to be larger than those of BL Lacs. Fig. 3 displays the F_{var} distribution of FSRQs and BL Lacs in J band. One can clearly see that J band F_{var}s of FSRQs are larger than those of BL Lacs. The difference is significant at a level of 5.7×10^{-4}.

We investigate the correlation between R and J bands. The R band versus J band is plotted in the left panels in Fig. 4. Linear fitting is carried out by the least square method (the solid line in the figure). In order to quantitatively search for the relation between these two bands, we calculate the correlation coefficient and estimate the significance level, and list them in Columns 7 and 8 of Table 1. From Fig. 4

Table 1 Continued.

Object	Class	ΔT (day)	N	J_{Fvar}	R_{Fvar}	r_{J-R}	Prob.	r_{C-R}	Prob.	r_{C-J}	Prob.	Behavior
PKS 1510-089	FSRQ	2207	405	0.96±0.03	0.85±0.03	0.96	$< 10^{-9}$	0.53	$< 10^{-9}$	0.74	$< 10^{-9}$	RWB
PKS 1514-241	BL Lac	1065	68	0.15±0.01	0.15±0.01	0.81	$< 10^{-9}$	-0.27	0.03	0.35	3.1×10^{-3}	RWB
PKS 1550-242	−	304	17	0.55±0.10	0.57±0.10	0.97	$< 10^{-9}$	-0.23	0.38	0.00	1.00	None
PMN J1610-6649	BL Lac	741	16	0.19±0.03	0.16±0.03	0.97	$< 10^{-9}$	0.53	0.03	0.72	1.8×10^{-3}	RWB
PKS 1622-253	FSRQ	988	6	0.46±0.13	0.48±0.15	0.74	0.09	-0.03	0.95	0.65	0.16	RWB
PKS 1622-297	FSRQ	2165	221	0.54±0.03	0.37±0.02	0.85	$< 10^{-9}$	0.27	4.9×10^{-5}	0.74	$< 10^{-9}$	RWB
1717-5156	−	455	133	0.88±0.05	0.39±0.02	0.86	$< 10^{-9}$	0.59	$< 10^{-9}$	0.92	$< 10^{-9}$	RWB
PKS 1730-130	FSRQ	1985	243	0.41±0.02	0.32±0.01	0.79	$< 10^{-9}$	-0.05	0.39	0.57	$< 10^{-9}$	RWB
OT 081	BL Lac	379	14	0.81±0.15	0.85±0.16	0.99	$< 10^{-9}$	-0.33	0.25	-0.19	0.51	None
PMN J1921-1607	BL Lac	543	13	0.28±0.06	0.23±0.05	0.96	2.3×10^{-7}	0.63	0.02	0.82	5.6×10^{-4}	RWB
PKS 1954-388	FSRQ	1118	54	0.42±0.04	0.29±0.03	0.96	$< 10^{-9}$	0.72	$< 10^{-9}$	0.88	$< 10^{-9}$	RWB
PKS 1958-179	FSRQ	919	18	1.09±0.18	1.17±0.20	0.98	$< 10^{-9}$	-0.59	0.01	-0.42	0.08	BWB
PKS 2052-474	FSRQ	1553	176	0.80±0.04	0.77±0.04	0.96	$< 10^{-9}$	0.10	0.18	0.39	7.8×10^{-8}	RWB
2FGL J2055.4 -0023	BL Lac	752	11	0.15±0.04	0.21±0.05	-0.29	0.38	-0.83	1.4×10^{-3}	0.77	5.4×10^{-3}	BWB(RWB)
PKS 2142-75	FSRQ	1316	157	0.52±0.03	0.17±0.01	0.88	$< 10^{-9}$	0.77	$< 10^{-9}$	0.98	$< 10^{-9}$	RWB
PKS 2149-306	FSRQ	158	22	0.17±0.03	0.09±0.01	0.92	2.0×10^{-9}	0.72	1.7×10^{-4}	0.94	$< 10^{-9}$	RWB
PKS 2155-304	BL Lac	1940	363	0.38±0.01	0.37±0.01	0.99	$< 10^{-9}$	0.06	0.29	0.22	1.7×10^{-5}	RWB
3C 446	BL Lac	1111	56	0.34±0.04	0.50±0.05	0.35	7.3×10^{-3}	-0.60	9.8×10^{-7}	0.53	2.2×10^{-5}	BWB(RWB)
PKS 2227-08	FSRQ	915	43	0.28±0.03	0.51±0.06	0.32	0.04	-0.87	$< 10^{-9}$	0.18	0.24	BWB
PKS 2232-488	FSRQ	661	10	0.41±0.09	0.26±0.06	0.66	0.04	0.02	0.96	0.76	0.01	RWB
PKS 2233-148	BL Lac	507	122	0.76±0.05	0.83±0.05	1.00	$< 10^{-9}$	-0.53	$< 10^{-9}$	-0.45	2.6×10^{-7}	BWB
PKS 2240-260	BL Lac	1147	20	0.24±0.04	0.22±0.04	0.92	1.1×10^{-8}	0.22	0.35	0.59	6.6×10^{-3}	RWB
3C 454.3	FSRQ	1985	505	0.90±0.03	0.81±0.03	0.99	$< 10^{-9}$	0.76	$< 10^{-9}$	0.85	$< 10^{-9}$	RWB
PKS 2255-282	FSRQ	947	42	0.57±0.06	0.49±0.05	0.94	$< 10^{-9}$	0.26	0.09	0.58	6.6×10^{-5}	RWB
1ES 2322-409	BL Lac	809	19	0.20±0.03	0.23±0.04	0.96	$< 10^{-9}$	-0.58	9.1×10^{-3}	-0.33	0.17	BWB
PKS 2326-502	FSRQ	128	76	0.58±0.05	0.72±0.06	0.97	$< 10^{-9}$	-0.56	1.8×10^{-7}	-0.35	2.2×10^{-3}	BWB
PMN 2345-1555	FSRQ	790	167	0.57±0.03	0.63±0.03	0.98	$< 10^{-9}$	-0.40	1.1×10^{-7}	-0.19	0.01	BWB
PKS 2345-16	FSRQ	372	22	0.81±0.12	0.79±0.12	-0.97	$< 10^{-9}$	-0.99	$< 10^{-9}$	0.99	$< 10^{-9}$	RWB(BWB)
H 2356-309	BL Lac	478	10	0.09±0.02	0.18±0.04	0.69	0.03	-0.83	3.1×10^{-3}	-0.16	0.65	BWB
4C+01.28	BL Lac	27	8	0.35±0.09	0.29±0.07	-0.95	3.5×10^{-4}	-0.99	4.6×10^{-6}	0.99	7.2×10^{-6}	BWB(RWB)

and the correlation coefficient, one can see that blazars show well-correlated variations between R and J bands, except for several sources showing weak or no, even negative correlations.

3 COLOR VARIATIONS

The color variability can reflect the spectral variability. Since these sources are highly variable, simultaneous or quasi-simultaneous observations are essential for color index calculation. The time series in the optical R band and the infrared J band are quasi-simultaneous and the best sampled in the SMARTS data. This provides us a chance to study in detail the spectral variations of the large sample of blazars on long time scales. $J - R$ color index is calculated pair by pair between R and J bands within the time interval of 15 minutes for each object. More than 90 percent of intervals are less than 5 minutes. Very few extremely strange data points have been discarded. The middle and right panels of Fig. 4 show the $J - R$ color variations with the brightness of R band and J band, respectively. To obtain the relation between the color index and the source brightness, we calculate the correlation coefficient r, and estimate the significance level. If $r >= 0.2$ and the significance level $p <= 0.01$, it means somewhat a good correlation between color index and magnitude. It suggests that the source becomes redder when the source becomes brighter. If $r <= -0.2$ and the significance level $p <= 0.01$, it means a well negative correlation, and suggests that the source tends to be bluer when the source is brighter. The other cases mean there is no correlation between color index and source brightness. Column 9 of Table 1 lists the correlation coefficient between the color index and the magnitude of R band (denoted by r_{C-R}). Its significance level is estimated and listed in Column 10. The correlation coefficient between the color index and the magnitude of J band (r_{C-J}) and its significance level are also calculated and listed in Columns 11 and 12. Overall, 43 sources (35 FSRQs, 7 BL Lacs and 1 unidentified object) show RWB trends and 24 sources (11 FSRQs, 11 BL Lacs and 2 unidentified objects) show BWB trends. There are
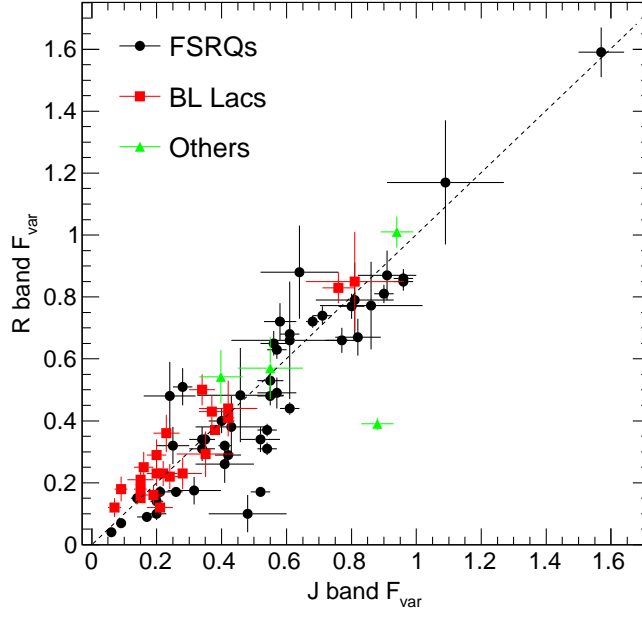
Fig. 1 F_{var}s of R band versus those of J band. The dots, squares and triangles represent FSRQs, BL Lacs and unidentified type objects, respectively. The dashed line means that the F_{var} of J band equal to that of R band.
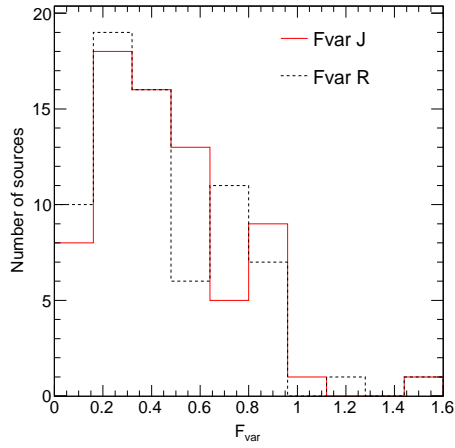

Fig. 2 Distributions of F_{vars} of the optical R band (the dashed line) and the infrared J band (the solid line).
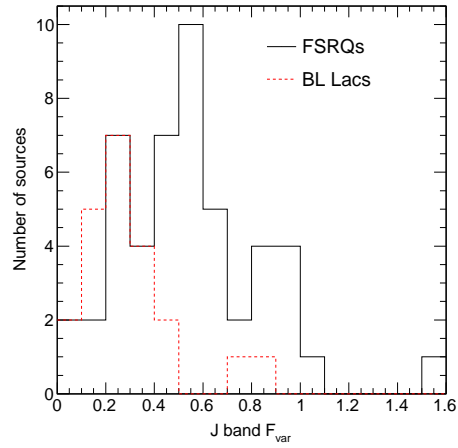
Fig. 3 Distributions of J band $F_{var}s$ of FSRQs (the solid line) and BL Lacs (the dashed line).

10 sources (6 FSRQs and 4 BL Lacs) showing BWB trends in the $Color - R$ plane and opposite trends in the $Color - J$ plane. The color behaviors are listed in Column 13 of Table 1.

4 DISCUSSION AND CONCLUSIONS

The BWB behavior is usually observed in BL Lac objects, which can usually be explained with shock-in-jet models. This behavior maybe means the presence of two components contributing to the overall emission, a variable component with a constant and relatively blue color and an underlying red component (Fiorucci et al. 2004; Ikejiri et al. 2011). RWB behavior is generally observed in FSRQs, which can be interpreted as due to a strong contribution of a blue thermal emission from the accretion disc, which mainly affects the bluer region of the optical spectrum when the jet emission is faint (Villata et al. 2006; Rani et al. 2010; Bonning et al. 2012).

An interesting result is that 10 sources show one color behavior in one band and an opposite trend in another band. When the R band (higher frequency) brightness increases, they tend to be BWB trends. However, they show RWB behavior when the source brightness increases in the J band (lower frequency). This phenomena had ever clearly appeared in the case of 3C 273 (Dai et al. 2009). This may be caused by the brightness variations in the higher frequency leading those in the lower frequency. In other words, the radiation emitted at higher frequencies will emerge sooner while the maximum flux at lower frequencies will be observed later (Villata et al. 2000; Papadakis et al. 2004; Villata et al. 2009; Zhang et al. 2010b; Rani et al. 2010). Thus the variations in lower frequencies can not keep step with those in high frequencies. One would observed weak or none, even negative correlations between the two bands. Therefore, the object exhibits BWB trend in the higher frequency band, while RWB trend in the lower frequency band. We check the brightness correlations between J and R bands, and find that the correlations are weak or negative for these sources.

For the sources with strong brightness correlations between R and J bands, their color behaviors in the R band are similar to those in the J band, showing either BWB or RWB behavior. We investigate the relation between color behavior and F_{var} difference of R and J bands for those objects with the absolute value of r_{J-R} greater than 0.5. In Fig. 5, we plot the r_{C-R} against the F_{var} difference, $F_{varR} - F_{varJ}$. Overall, if F_{var} of R band is greater than that of J band, $r_{C-R} < 0$, which means the source showing BWB trend. If F_{var} of R band is less than that of J band, the source shows RWB trend ($r_{C-R} > 0$).
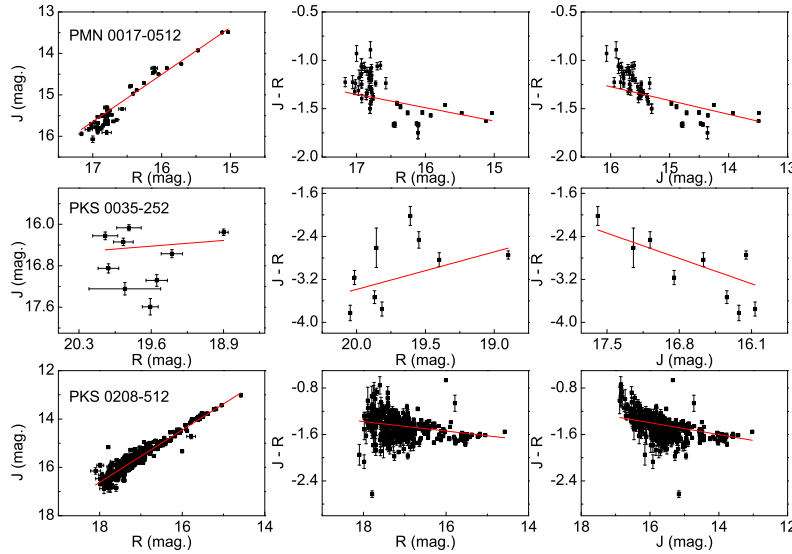

Fig. 4 Left: Relations between the J and R magnitudes. Middle: Color index versus the magnitude of R band. Right: Color index versus the magnitude of J band. The solid lines represent the best linear fitting.
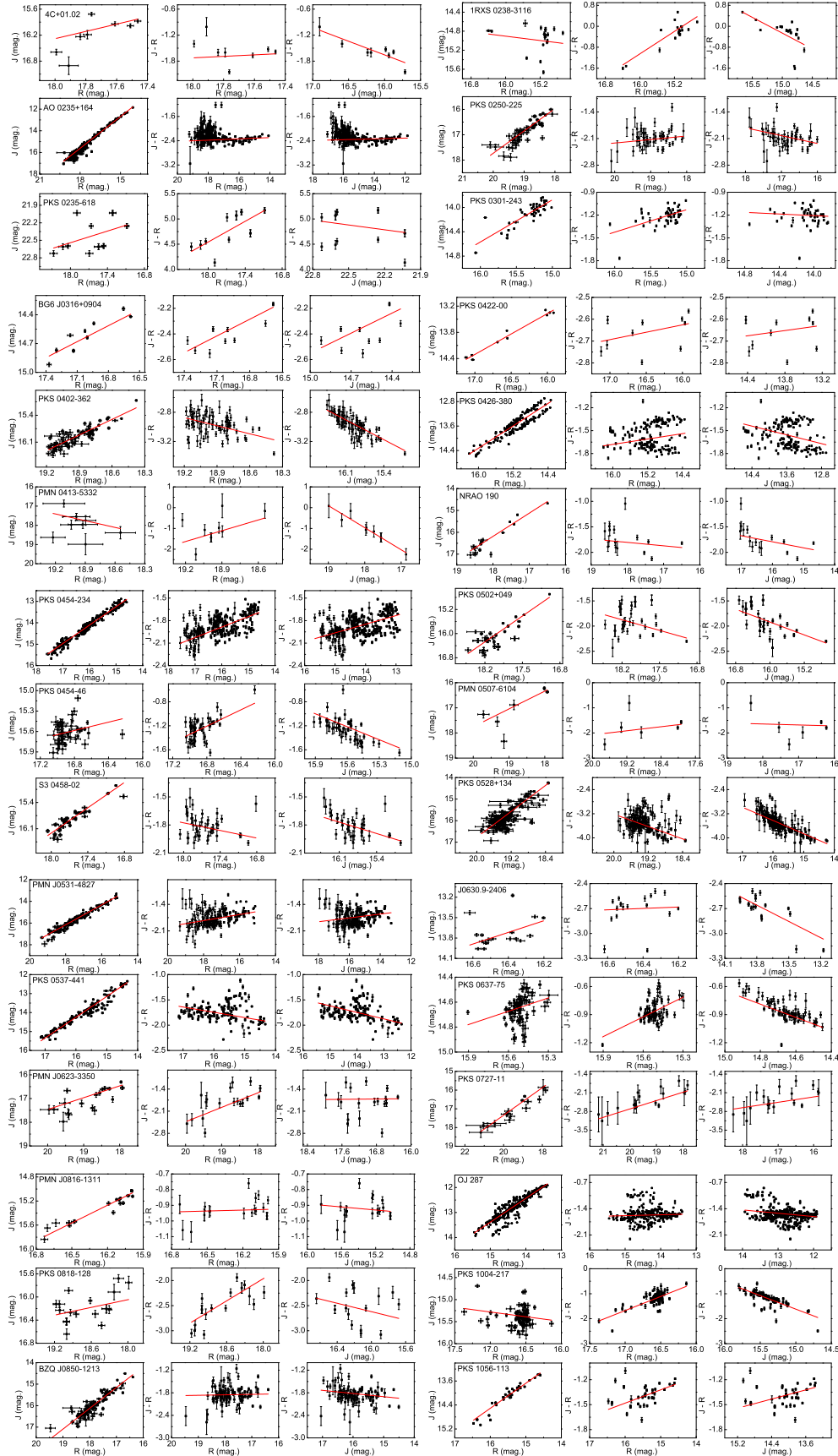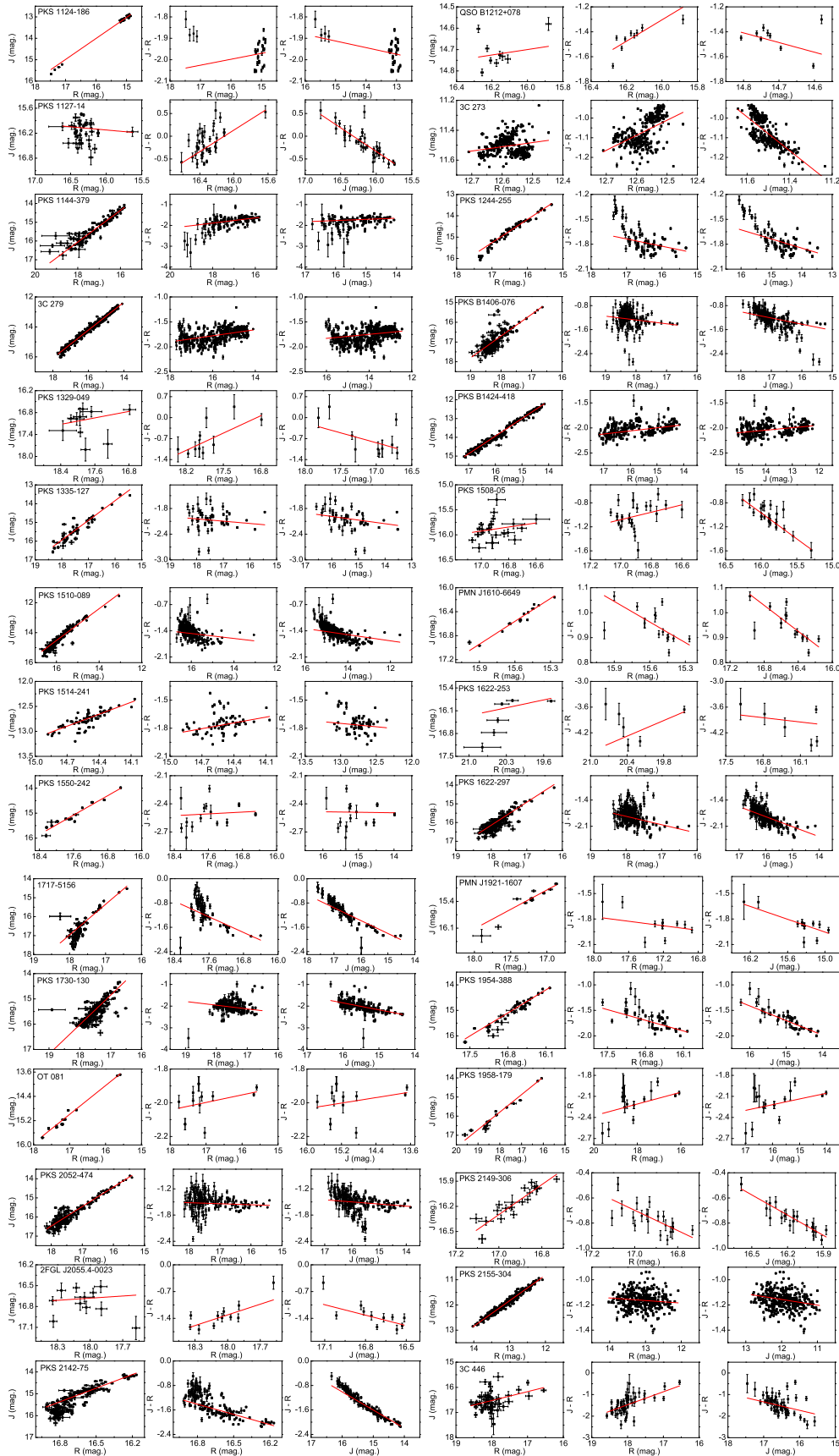
Fig. 4 Continued.
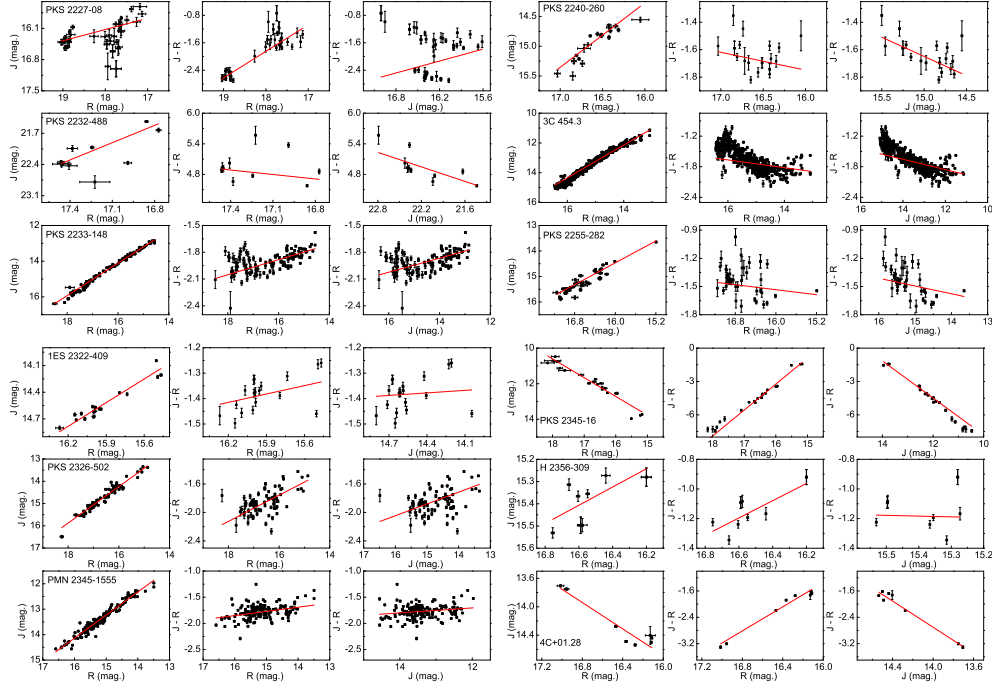
Fig. 4 Continued.

Fig. 4 Continued.

This means that the difference in variation amplitude can cause different color behaviors. For an object with the fluxes at different frequencies varying simultaneously, if the amplitude is larger at the higher frequency than at the lower one, it exhibits the BWB trend. Oppositely, the larger amplitude variations at lower frequency can result in RWB trend.

From Fig. 4, one can see that not all sources can be fitted well by a straight line. The color variation of some sources maybe change trend at a certain magnitude. Several sources show RWB in the low state, and then keep a stable trend in the high state (SWB), such as PMN 0017−0512, PKS 0208−512, PKS 1244−255, PKS 1510−089, PKS 1622−297 and 1717−5156. Some sources show RWB trend in the low state, and BWB trend in the high state, like AO 0235+164, PKS 1056-113, PKS 2233-148, PKS 2240-260 and 3C 454.3. This behavior has also been found in other literature, such as 3C 454.3, PKS 1510-089, PG 1553+113 and PKS 0537-441 in Villata et al. (2006), Ikejiri et al. (2011) and Zhang et al. (2013). Most of these sources are FSRQs. They have a common feature that they exhibit RWB trend in the faint state and then SWB or BWB trend in the bright state. This may be explained as the contribution reversal of different emission components. In the faint state, the strong contribution of thermal emission from an accretion disk results in RWB trend. While in the bright state, the non-thermal jet emission is dominant, which would display usual BWB trend, therefore balancing or exceeding the RWB trend. Thus, the source transforms its color behavior from RWB trend to SWB or BWB trend.

A few sources show two or more different strips in the $Magnitude - Magnitude$ or $Color - Magnitude$ diagrams. PKS 0426-380 shows two clear different behaviors. In $J - R$ diagram, it seems to be a gap of two light curves with different traces. In the $Color - Magnitude$ diagram, there is also an intersection of two curves. One exhibits BWB trend, and another exhibits RWB trend. OJ 287 indicates two parts in the color behavior, and the data points are very scattered. The color seems to be no trend in the $Color - R$ diagram, however, show a slight RWB trend in the $Color - J$ diagram. The BWB trend had been found in this source (Vagnetti, Trevese & Nesci 2003; Fiorucci et al. 2004; Wu et al. 2006; Dai et al. 2011). A tendency to move around a circle in $Color - Magnitude$ diagram was also found by
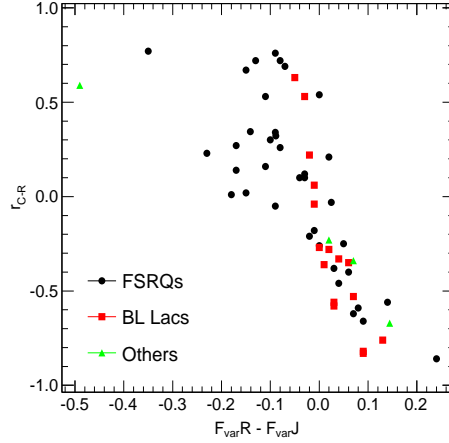
Fig. 5 Correlation coefficient r_{C-R} versus the F_{var} difference of R and J bands.

Bonning et al. (2012) and Sandrinelli, Covino & Treves (2014). For the 3C 273, $J - R$ plot shows two separative parts, and the $Color - Magnitude$ plot also shows two separative parts. Two parts both have a RWB trend, and totally, $Color - J$ show RWB trend. However, in $Color - R$ plot, the combination of two part shows BWB trend. Very recently, Fan et al. (2014) also found that this source exhibited two separative parts in the plot of spectral index versus flux density. PKS 2052-474 seems to display two different behaviors in the variations both with RWB trends. PKS 2227-08 shows two separative parts, which both show RWB trend. However, the combination of two parts shows a BWB trend in $C - R$ plot. These color behaviors are puzzling, which suggest that there maybe exist more complicated and separative emission components in these sources.

In conclusion, the color variability has been investigated with a large sample of blazars in optical and infrared region. On the whole, 46 out of 49 FSRQs show color variations with RWB trends (35 FSRQs) or BWB trends (11 FSRQs), and 18 out of 22 BL Lacs show RWB trends (7 BL Lacs) or BWB trends (11 BL Lacs). Among them, 10 blazars follow RWB trend in the faint state and then SWB or BWB trend in the bright state.

References

Arévalo P., Uttley P., Kaspi S., Breedt E., Lira P., & McHardy I. M., 2008, MNRAS, 389, 1479
Bonning E., Urry C. M., Bailyn C., et al., 2012, ApJ, 756, 13
Carini M. T., Miller H. R., Noble J. C., & Goodrich B. D., 1992, AJ, 104, 15
Chatterjee R., Bailyn C. D., Bonning E. W., et al., 2012, ApJ, 749, 191
Ciprini S., Takalo L. O., Tosti G., et al., 2007, A&A, 467, 465
D'Ammando F., Antolini E., Tosti G., et al., 2013, MNRAS, 431, 2481
Dai B. Z., Li X. H., Liu Z. M., et al., 2009, MNRAS, 392, 1181
Dai Y., Wu J., Zhu Z. H., Zhou X., & Ma J., 2011, AJ, 141, 65
Fan J. H., & Lin R. G., 2000, ApJ, 537, 101
Fan J. H., Kurtanidze O., Liu Y., Richter G. M., Chanishvili R., & Yuan Y. H., 2014, ApJS, 213, 26
Fiorucci M., Ciprini S., & Tosti G., 2004, A&A, 419, 25

Gaur H., Gupta A. C., Strigachev A., et al., 2012, MNRAS, 425, 3002
Ghosh K. K., Ramsey B. D., Sadun A. C., & Soundararajaperumal S., 2000, ApJS, 127, 11
Gu M. F., Lee C. U., Pak S., Yim H. S., & Fletcher A. B., 2006, A&A, 450, 39
Gu M. F., & Ai Y. L., 2011, A&A, 528, 95
Hu S. M., Wu J. H., Zhao G., & Zhou X., 2006, MNRAS, 373, 209
Ikejiri Y., Uemura M., Sasada M., et al., 2011, PASJ, 63, 639
Papadakis I. E., Boumis P., Samaritakis V., & Papamastorakis J., 2003, A&A, 397, 565
Papadakis I. E., Samaritakis V., Boumis P., & Papamastorakis J., 2004, A&A, 426, 437
Raiteri C. M., Villata M., Tosti G., et al., 2003, A&A, 402, 151
Rani B., Gupta A. C., Strigachev A., et al., 2010, MNRAS, 404, 1992
Sandrinelli A., Covino S., & Treves A., 2014, A&A, 562, A79
Vagnetti F., Trevese D., & Nesci R., 2003, ApJ, 590, 123
Vaughan S., Edelson R., Warwick R. S., & Uttley P., 2003, MNRAS, 345, 1271
Villata M., Mattox J. R., Massaro E., et al., 2000, A&A, 363, 108
Villata M., Raiteri C. M., Balonek T. J., et al., 2006, A&A, 453, 817
Villata M., Raiteri C. M., Larionov V. M., et al., 2009, A&A, 501, 455
Wu J., Zhou X., Ma J., & Jiang Z., 2011, MNRAS, 418, 1640
Wu J., Zhou X., Wu X. B., et al., 2006, AJ, 132, 1256
Zhang B. K., Dai B. Z., Zhang L., & Cao Z., 2010a, RAA, 10, 653
Zhang B. K., Dai B. Z., Zhang L., Liu J. L., & Cao Z., 2010b, PASA, 27, 296
Zhang B. K., Wang S., Zhao X. Y., Dai B. Z., & Zha M., 2013, MNRAS, 428, 3630
Zhang B. K., Zhao X. Y., Wang C. X., & Dai B. Z., 2014, RAA, 14, 933